

Electronic dispersion relations of monolayer hexagonal boron nitride formed on the Ni(111) surface

A. Nagashima, N. Tejima, Y. Gamou, T. Kawai, and C. Oshima

Department of Applied Physics, Waseda University, 3-4-1 Okubo, Shinjuku-ku, Tokyo 169, Japan

(Received 11 October 1994)

Angle-resolved ultraviolet-photoelectron spectroscopy and angle-resolved secondary-electron emission spectroscopy have been carried out for a film of single-crystalline hexagonal boron nitride (*h*-BN) formed on the Ni(111) surface to investigate both the valence- and conduction-band structures. The thickness of the film studied in this experiment was 1 ML. The observed electronic dispersion relations were compared with some theoretical ones reported for bulk *h*-BN. Among these theoretical calculations, the one by Catellani *et al.* [Phys. Rev. B **36**, 6105 (1987)] is in the best agreement with the present results. We have discussed the strength of the interfacial bond and the influence of this bond upon the electronic states of the monolayer *h*-BN film on the basis of the observed band structures for the BN film and a film of monolayer graphite formed on Ni(111).

I. INTRODUCTION

In recent years, much attention has been devoted to boron nitride (BN) in relation to its technological applications.¹ From a fundamental scientific point of view, hexagonal BN (*h*-BN) is an attractive highly anisotropic insulating material isostructural to semimetallic graphite.^{2,3} While there is good agreement between the various theoretical band calculations and experimental results for graphite,⁴⁻⁷ such consensus has not been achieved for *h*-BN in spite of the structural similarity. As for the widths of the π bands, which are important for the electronic and optical properties, for instance, various different calculated values have been presented, ranging from 1.2 to 9.3 eV.⁸⁻¹⁴ The reason why such a large discrepancy has arisen is mainly ascribed to the lack of precise experimental data concerning the band structure, with which the theoretical results can be evaluated. Although some papers have reported the experimental density of states for the valence electrons,^{3,15,16} as far as we know, no experimental dispersion relations of the energy bands in *h*-BN have been presented to date. This was due to the nonavailability of single-crystalline samples large enough for angle-resolved electron spectroscopy measurements.

In this experiment, we have observed both the valence- and conduction-band structures of a film of single-crystalline BN on the Ni(111) surface by using angle-resolved ultraviolet-photoelectron spectroscopy (ARUPS) and angle-resolved secondary-electron-emission spectroscopy (ARSEES). The thickness of the film prepared by thermal decomposition of borazine ($B_3N_3H_6$) was 1 ML. The present results are compared with some theoretical band structures available at present and possible reasons for the agreement and disagreement among them are discussed. Here, one may object that the validity of the calculations cannot necessarily be evaluated properly by comparison with the observed band structure of the monolayer BN film in contact with the metal surface,

since the electronic structure of the film could be modified by the interaction with the substrate. Indeed, in previous work, we have observed such modification of the band structure of a monolayer graphite (MG) film formed on the (111) surfaces of Ni and some transition-metal carbides.¹⁷⁻¹⁹ These results implied that a similar deformation of the band structure could occur in the monolayer BN film. However, as will be clarified in this paper, the bond between the BN film and the Ni(111) surface is much weaker compared with that between MG and the same substrate. This striking contrast is attributed to the difference in the electronic structure; while graphite is a semimetal, BN is an insulator with a wide band gap. As a consequence, at least for the first-order approximation, the band structure of the BN film on the metal surface could be regarded as that of the isolated solid monolayer.

II. EXPERIMENT

The experiments were done in a two-level ultrahigh-vacuum (UHV) chamber with a base pressure of $\sim 1 \times 10^{-8}$ Pa. The chamber was equipped with low-energy electron-diffraction (LEED) optics; an ion-bombardment gun; two gas inlets for dosing borazine and ethylene gases in the upper stage; a hemispherical energy analyzer; an ultraviolet discharge lamp; an x-ray source; and an electron gun in the lower stage. The unpolarized He I ($h\nu=21.2$ eV) and He II (40.8 eV) resonance lines were used for ARUPS and the characteristic x-rays of Mg $K\alpha$ (1253.6 eV) and Al $K\alpha$ (1486.6 eV) were used for x-ray photoelectron spectroscopy (XPS). For the ARUPS and XPS measurements, the analyzer was set to have the resolution of 0.2 and 0.5 eV, respectively. Since the linewidths of the Mg $K\alpha$ and Al $K\alpha$ x-rays are 0.7 and 0.8 eV, the overall energy resolution for the XPS measurements was about 0.9 ± 0.04 eV. In the ARSEES measurements, primary electrons were impinged onto the sample surface with an incident angle of 43° . The typical specimen current was 1 nA. In order to confirm that the observed peaks in the ARSEES spectra were not due to

the inelastically scattered incident electrons but due to the secondary electrons emitted from the sample, several primary energies were chosen in the range from 60 to 110 eV. For the ARSEES measurement, the energy resolution of the analyzer was set to be 0.2 eV. The substrate used in this experiment was a Ni(111) surface. One face of the specimen was mechanically polished and chemically etched. In the UHV chamber the specimen was further cleaned by repeated cycles of Ar-ion sputtering and annealing at about 800°C. After these procedures, the LEED pattern of the clean surface showed sharp diffraction spots in a low background, corresponding to a (1×1) atomic structure. No impurities such as sulfur or carbon were detected in the XPS spectra. The monolayer graphite film was deposited on the substrate by thermal decomposition of ethylene gas. The precise conditions for the preparation of the MG were described elsewhere.⁹

For preparing BN films of good crystallinity, the use of borazine as a precursor is very effective since this molecule has the clear advantage that the B:N stoichiometry is 1:1. Borazine reagent with a purity of 98% was purchased from ADCS, Inc. The liquid borazine was loaded into a cylinder together with nitrogen gas and was stored in a freezer at a temperature under -20°C in order to prevent decomposition. Prior to borazine introduction, almost the entire dosing line except the part in the freezer was thoroughly degassed by baking at 150°C for 24 h. Every 12 h after charging the line and doser with borazine gas, they were evacuated and charged again. As in the case of water, borazine gas was introduced into the UHV chamber through a narrow tube and the sample was set closer to the end of the tube during the exposure to limit borazine adsorption onto the inner wall of the chamber. Therefore the amounts of borazine exposure reported in units of langmuirs (1 L = 1 × 10⁻⁶ Torr sec) are only semiquantitative due to the absence of correction for doser enhancement of sample position and cointroduction of nitrogen gas into the chamber.

III. RESULTS AND DISCUSSION

A. Growth of *h*-BN film

The single-crystalline *h*-BN overlayer was epitaxially grown by decomposition of borazine gas on the substrate at 800°C. To form the monolayer *h*-BN, an exposure of 100 L was necessary. A sharp (1×1) LEED pattern of the sample showed a commensurate relation between the monolayer BN and the substrate. This seems reasonable since the in-plane lattice constant of the bulk *h*-BN, 2.50 Å is very close to that of the Ni(111) surface, 2.49 Å. Upon the formation of the overlayer, additional B 1s and N 1s peaks appeared in the XPS spectrum at the binding energies of 191.2 and 399.1 eV, respectively. The full widths at half maxima for these peaks (1.4 eV) were identical with those for the C 1s peaks of the graphite and the monolayer graphite film formed on the Ni(111) surface. Together with the sharp LEED pattern, this fact indicates that the *h*-BN film prepared by the present method has good crystalline quality comparable to that of the graphite.

Figure 1 shows the intensity of the N 1s XPS peak for

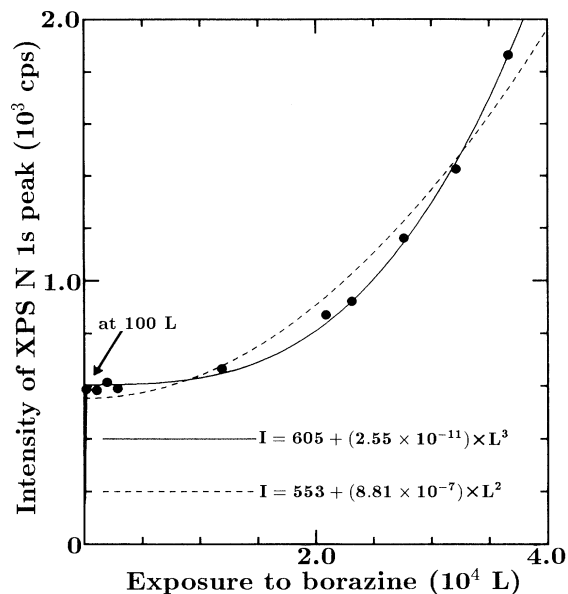


FIG. 1. Change in the intensity of the XPS N 1s peak for the BN film as a function of borazine exposure with the substrate temperature of 800°C. The solid (broken) curve illustrates the phenomenological equation obtained by using a least-squares method with the assumption that after the first monolayer formation the growth of the BN is proportional to the third (second) power of the exposure.

the BN film as a function of borazine exposure with the substrate temperature at 800°C. While the growth of the first monolayer of BN was quickly accomplished, the growth rate of the following layers was much slower; to form additional 1-ML equivalents, an exposure of 2.9×10^4 L was necessary, which was about 300 times as large as the exposure necessary for the first monolayer formation. This is related to the fact that the chemical reactivity of the surface for borazine decomposition is strongly reduced by the monolayer BN coating.²⁰ It should be noted that the growth of the BN did not proceed in a layer-by-layer fashion after the formation of the first monolayer but that it grew in the Stranski-Krastanov mode. As the intensity of the N 1s peak increased beyond the value of the monolayer film, the LEED pattern of the sample became diffuse with broad spots in a high background. Moreover, besides the peaks of the π and σ bands, additional dispersionless peaks appeared in the ARUPS spectra and the relative intensities of these peaks to the π and σ peaks increased monotonically with increase in N 1s peak. These results strongly suggest that the BN film has not grown in a two-dimensional fashion but that three-dimensional (3D) clumps have begun to form on the first monolayer.

It is clearly seen from Fig. 1 that the growth rate of the BN became larger with increase in the exposure. This could be ascribed to the increase in the surface area or the steps (*S*) of the 3D clumps, which might be related to the decomposition of the borazine molecules. In Fig. 1,

the solid curve illustrates the phenomenological equation obtained by using a least-squares method with the assumption that after the first monolayer formation the growth of the BN is proportional to the third power of the exposure. Compared to the broken curve in Fig. 1 which was calculated with the second-power assumption, the solid curve agrees quite well with the experimental data, exhibiting a very small deviation. At present, we tentatively explain this phenomenon as follows. The small change in the total volume of the 3D clumps (dV) is proportional to SdL , where dL stands for the small increase in the exposure. Roughly speaking, S is proportional to $V^{2/3}$. Then it follows that $V^{1/3} \propto L$. Therefore the observed intensity of the N 1s peak is proportional to the third power of the exposure as shown in Fig. 1.

B. Dispersion curves of valence-band structure

Figures 2(a) and 2(b) show the typical ARUPS spectra of the monolayer h -BN/Ni(111) measured for the $\Gamma\bar{K}$ symmetry axis of the two-dimensional Brillouin zone with photon energies of 21.2 and 40.8 eV, respectively. The emission angle referred to the surface normal is indicated for each spectrum. In Fig. 2(a), there are several peaks besides those for the π and σ bands of the BN. The almost dispersionless peaks near the Fermi level (E_F) are due to emission from the d bands of the Ni substrate. The other peaks in the higher-binding-energy region with relatively high intensities are ascribed to the emission of secondary electrons for the following reasons. First, these peaks do not have corresponding ones in Fig. 2(b) obtained with higher photon energy, which suggests that they do not represent the occupied electronic states directly. Second, as shown later in the following section, the energy dispersions of these peaks agree well with those of some of the peaks observed in the ARSEES spectra.

In Fig. 3, we plotted the binding energies (E_B) of the observed photoemission peaks in the ARUPS spectra of the monolayer h -BN/Ni(111) system versus the wave vector parallel to the surface (k_{\parallel}) obtained by using the following formula:

$$k_{\parallel} = [2m(h\nu - \phi - E_B)/\hbar^2]^{1/2} \sin\theta, \quad (1)$$

where m is the rest mass of the electron, $h\nu$ the photon energy for excitation, ϕ the work function of the system (3.6 ± 0.1 eV, determined in the present work), and θ the emission angle referred to the surface normal. Open and solid circles represent the data obtained with He I and He II resonance lines, respectively. The theoretical energy band structure¹⁴ of the bulk h -BN is also indicated by broken curves for comparison, where the theoretical valence-band maximum (VM) is placed at the binding energy of 4.0 eV to fit the theoretical band structure to the experimental one. The shaded bands represent the dispersion curves of the d bands observed for the clean Ni(111) surface with a photon energy of 21.2 eV. Almost all the branches near E_F observed for the BN-covered Ni(111) surface agree well with those for the clean surface. In Fig. 3, along the $\Gamma\bar{M}$ direction, there is a branch at ~ 1 eV, of which the corresponding one for the clean

surface is not depicted. This is due to the very steep Fermi cutoff in the ARUPS spectrum for the clean surface, where the tail has obscured the existing structure at around 1 eV and made it impossible to assign the precise

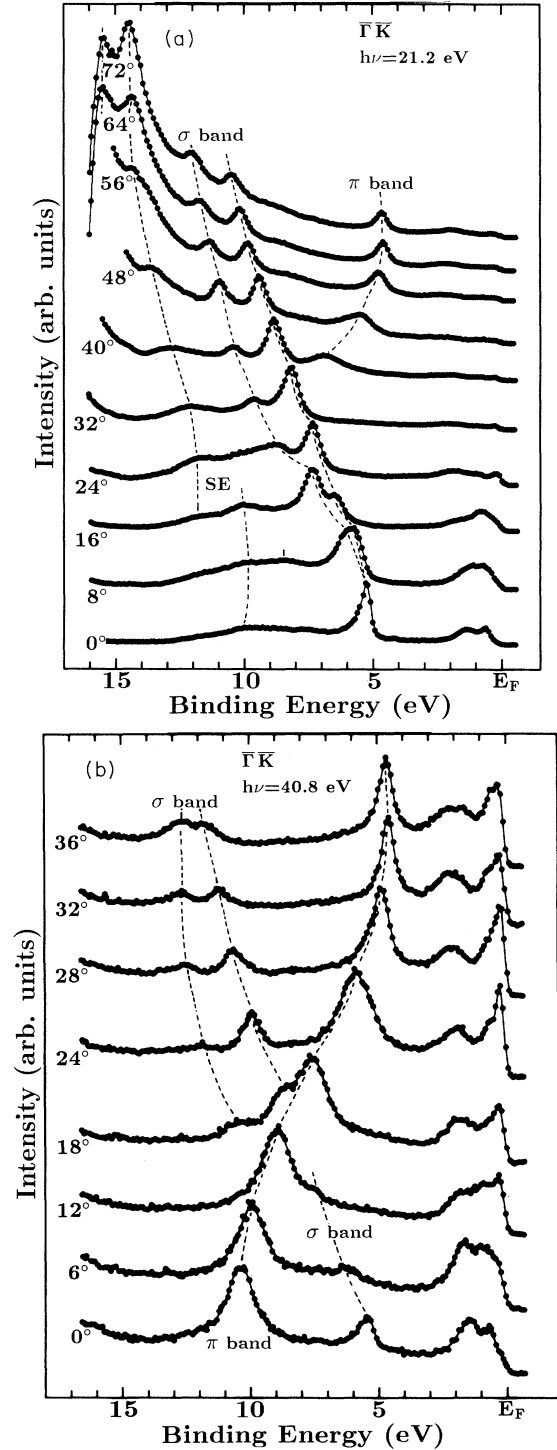


FIG. 2. Typical ARUPS spectra of the monolayer h -BN/Ni(111) excited by (a) He I ($h\nu = 21.2$ eV) and (b) He II (40.8 eV) resonance lines, respectively. The polar angle of emitted electrons is denoted for each spectrum. SE is an abbreviation for secondary electron.

TABLE I. Experimental and theoretical values (in eV) for the widths of the valence bands and for the difference between the maxima of the π and σ bands. σ_1 and σ_2 denote the higher and lower σ bands, respectively.

	Width of π band	Width of σ_1 band	Width of σ_2 band	π - σ energy difference
Experimental	5.8	6.5	8.2	0.9
Nakhmanson and Smirnov (Ref. 9)	7.5,9.3	8.7	9.2,10	4.9,5.8
Zupan (Ref. 11)	3.2,3.5	4.5	6.3	0.7
Zunger, Katzir, and Halperin ^a (Ref. 12)	4.6	3.1	4.2	2.1
Robertson (Ref. 13)	4.9,6.0	6.2	9.0	3.0
Catellani <i>et al.</i> (Ref. 14)	4.3,6.7	6.2	7.4	1.7,2.1

^aCalculated with modified iterated extended Hückel method.

energy of this structure.

In Table I, we tabulate the observed values of the widths of the valence bands and the difference in energy between the maxima of the π and σ bands. σ_1 and σ_2 denote the higher and lower σ bands, respectively. In Table I, these experimental results are compared with the five band calculations presented by Nakhmanson and Smirnov,⁹ Zupan,¹¹ Zunger, Katzir, and Halperin,¹²

Robertson,¹³ and Catellani *et al.*¹⁴ Since all of these calculations except the one by Zunger, Katzir, and Halperin were performed for bulk *h*-BN, some of the energy bands are split due to the interlayer interaction. Therefore some of the spaces in Table I show double values. In Ref. 12, the energy bands of an isolated monolayer *h*-BN film were calculated with three different methods, among which the modified iterated extended Hückel method gave relatively good agreement with the present results.

It is clearly seen from Table I that the results of Nakhmanson and Smirnov with the orthogonalized-plane-wave (OPW) method do not agree well with the present results. For instance, the calculated widths of the π bands are 7.5 and 9.3 eV, of which the average is larger than the present experimental value by 2.4 eV. In addition, the difference in energy between the maxima of the π and σ bands (4.9 eV) is much larger than the present value (0.9 eV). Such a large value is also inconsistent with the experimental density of states for transitions from the π and σ bands to the B 1s core hole measured by *K* emission spectroscopy.³ Next, we examine the results of Refs. 11–13 which were calculated with a tight-binding (TB) approximation. While the calculated bandwidths by Robertson agree well with the experimental ones, the works by Zupan and Zunger, Katzir, and Halperin have underestimated these values in spite of using the same calculation method. This contrast could be ascribed to the choice of the more realistic TB parameters in Robertson's work,¹³ although it shows rather poor agreement with the experiments concerning the energy difference between the π and σ bands.

Among the five calculations listed in Table I, the one by Catellani *et al.*¹⁴ shows the best agreement with the experimental band structure. The agreement concerning both the bandwidths and the energy difference is good in comparison with the other calculations. In addition to this, it is only the band calculation in Ref. 14 that reproduces the observed feature described below; as shown in Fig. 3, the downward dispersion of the lower σ band along the $\bar{\Gamma}\bar{K}$ direction changes to an upward one at the point where the wave vector k_{\parallel} is about 1.4 \AA^{-1} . In view

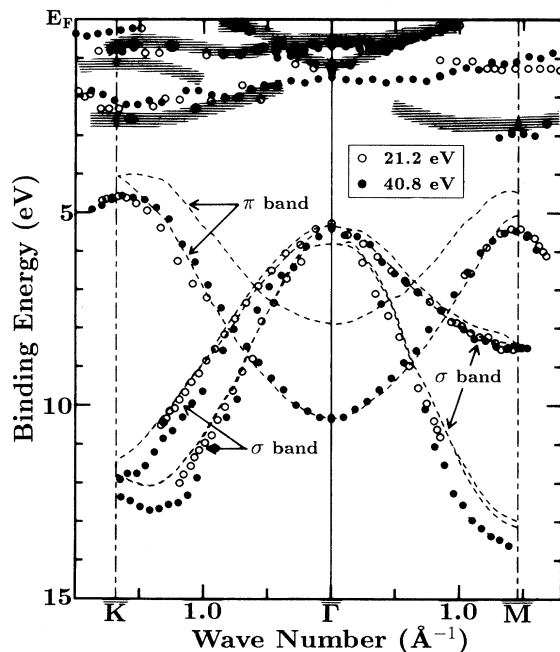


FIG. 3. Experimental valence-band structure of the monolayer *h*-BN/Ni(111). Open (solid) circles denote the data obtained with He I (He II) resonance line. Shaded bands with horizontal lines near E_F indicate the dispersion relations of the *d* bands for the clean Ni(111) surface measured with He I. The theoretical band structure of bulk *h*-BN (Ref. 14) is also indicated by broken curves for comparison, where the theoretical valence-band maximum is set to have the binding energy of 4.0 eV to make a good fit with the experimental data.

of the fact that the first four calculations were done with non-self-consistent potentials and small basis sets, such as 16 atomic orbitals and 73 OPW's, the good agreement between the experiment and the latest calculation demonstrates that all-electron full-potential self-consistent calculations with large basis sets (e.g., about 250 augmented plane waves used in Ref. 14) are desirable for describing the band structure of *h*-BN precisely, even for the description of the valence-band structure.

Despite the fairly good agreement, at the same time there are some discrepancies between the results of Ref. 14 and the present work. First, the theoretical widths of all the bands are slightly smaller than the experimental values. This might stem from the underestimation of the theory about the in-plane bond, although we could not completely rule out the possibility that the small contraction of the lattice constant of the BN film for matching with the periodicity of the Ni(111) surface widens the valence bands. Second, if the value for the gap between the bonding π and antibonding π^* bands in the films is similar to the calculated one for bulk BN (3.9 eV), part of the π^* band could be observed under E_F since the experimental VM has a binding energy of 4.6 eV. However, we have not detected such a metallic band in the BN film. In fact, the authors of Ref. 14 mentioned that the use of the local-density approximation underestimates the values of energy gaps. Furthermore, the experimental values for the energy gap in the bulk BN measured by several methods well exceeded the calculated value.^{12,21-23} Therefore we conclude that the monolayer *h*-BN film on the Ni(111) surface is an insulating material with a band-gap energy over 4.6 eV.

C. Dispersion curves of conduction-band structure

Figure 4 shows typical ARSEES spectra of the monolayer *h*-BN/Ni(111) system observed for the $\bar{\Gamma}\bar{M}$ symmetry axis with a primary energy for the incident electrons of 70 eV. The emission angle is denoted for each spectrum. In comparison with the lower-energy parts of the spectra, the higher parts in the energy region above 12 eV are drawn with larger scales because of the much weaker intensities. In Fig. 5, we plotted the energy positions (E_C) of the observed secondary-electron peaks in the ARUPS spectra measured with a photon energy of 21.2 eV and the ARSEES spectra versus the wave vector parallel to the surface (k_{\parallel}) obtained by using the following formula:

$$k_{\parallel} = [2m(E_C - \phi)/\hbar^2]^{1/2} \sin\theta, \quad (2)$$

where E_C is the energy relative to E_F . Open and solid circles represent the data acquired from the ARUPS and ARSEES measurements, respectively. Since the lowest-energy peak in Fig. 4 indicated by the dash-dotted curve is excluded from the experimental conduction-band structure of the film drawn in Fig. 5.

In Fig. 5, the theoretical conduction-band structure for bulk *h*-BN is also indicated by shaded bands, where the broken curves represent the interlayer states.¹⁴ Because of the monolayer thickness of the film, such inter-

layer states have not been observed, of course, in the present study. Note that, among the band calculations listed in Table I, only that of Ref. 14 is available for comparison with the experimental band structure over the wide energy range from the vacuum level (E_V) to 22 eV above E_F . As shown in Fig. 5, the theoretical band structure corresponds well with the experimental data. Especially, the observed lowest branch is excellently reproduced by the calculation and, with the help of the theoretical work, the observed splitting of this branch for the $\bar{\Gamma}\bar{M}$ direction is explained as the σ - π splitting of the bands.

In Fig. 5, all the theoretical conduction bands were shifted in order to make a good fit with the experimental data, namely, the theoretical conduction-band minimum was placed at the energy of 2.7 eV above E_F . Accordingly, the band gap in the monolayer *h*-BN film is roughly estimated to be ~ 7 eV, since the experimental VM was found at the binding energy of 4.6 eV. Compared to the experimental values for the band gap in bulk BN measured by several methods,^{12,21-23} which were in the range of 5–6 eV, the above estimated values seems to be somewhat large. This discrepancy might be due to the final-state effect in the ARUPS measurement; because a hole left after photoemission is not fully screened by conduction electrons in the insulating film, the binding energies

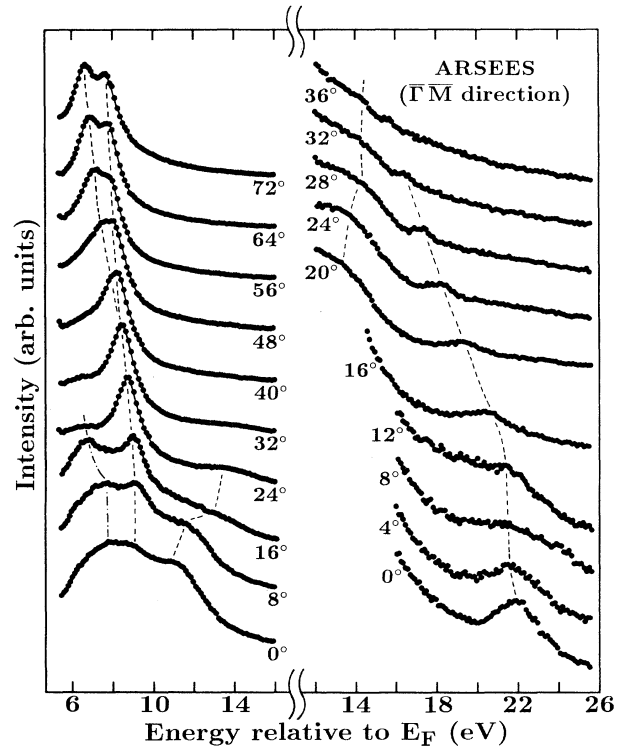


FIG. 4. Typical ARSEES spectra of the monolayer *h*-BN/Ni(111) observed with a primary energy for incident electrons of 70 eV. The polar angle of emitted electrons is denoted for each spectrum.

of the valence bands tend to be overestimated. A similar mechanism has been employed to explain the difference in the value for separation of highest occupied and lowest unoccupied molecular orbitals (HOMO-LUMO separation) in solid C_{60} between the band calculation and experiments performed by using photoemission and inverse photoemission spectroscopy.²⁴ Therefore we infer that the band gap in the monolayer BN film (E_G in eV) is $4.6 < E_G \lesssim 7$.

D. Comparison with monolayer graphite film

The present results on both the valence and conduction bands suggest that the electronic structure of the monolayer BN film is very similar to that of bulk BN, implying weak interaction between the film and the metal substrate. In fact, as shown in Figs. 2 and 3, the binding energies of the valence bands of the BN film are deeper than those of the d bands of the substrate by, at least, 2 eV. Because of this difference in energy, mixing of the electronic states of the overlayer with those of the substrate seems unfavorable. To gain a better understanding of the interfacial bonding between the overlayer and the metal surface, a comparison between the band structures of the monolayer BN/Ni(111) system and the MG/Ni(111) system is of great value.

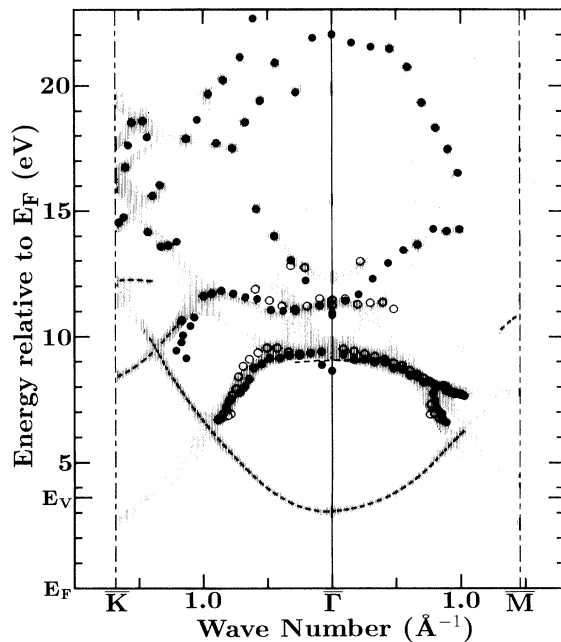


FIG. 5. Experimental conduction-band structure of the monolayer h -BN/Ni(111). Open and solid circles denote the data acquired from the ARUPS spectra measured with a photon energy of 21.2 eV and the ARSEES spectra, respectively. Shaded bands indicate the theoretical conduction-band structure (Ref. 14), where the broken curves represent the interlayer states. The theoretical conduction-band minimum is placed at the energy of 2.7 eV above E_F to make a good correspondence with the experimental data.

Figure 6 shows typical ARUPS spectra of MG/Ni(111) measured for the $\bar{\Gamma}\bar{K}$ symmetry axis with a photon energy of 40.8 eV. As is clear from Figs. 2(b) and 6, the ARUPS spectra of the BN film and MG exhibit several similarities in shape; the intense π peak with large energy dispersion, the two less intense σ peaks, and the almost dispersionless peaks near E_F . This is attributed to the analogous structures of these two materials. At the same time, however, some differences should be noted. The width of the π band in MG is larger than that of the π band in the BN film by 1.8 eV, which is ascribed to the fact that, while the bond between the B and N atoms in BN is partially ionic due to the difference in electronegativity,^{14,25} the bond between the neighboring C atoms in graphite is perfectly covalent. Because of this larger dispersion, the π peak of MG gets closer to the substrate peaks near E_F with increase in the emission angle, and these peaks begin to form a broad continuum as shown in Fig. 6. This strongly suggests that a mixing of the π states with the d states of the substrate can occur, which is not the case for the monolayer h -BN/Ni(111) system.

Figure 7 shows the experimental band structure of the MG/Ni(111) system. The branch due to the emission of secondary electrons¹⁸ is indicated by the shaded band with vertical lines. The broken curves indicate the corresponding experimental band structure of bulk graphite.⁶ The observed band structure of MG is different from the bulk one in the following two features. First, while the σ

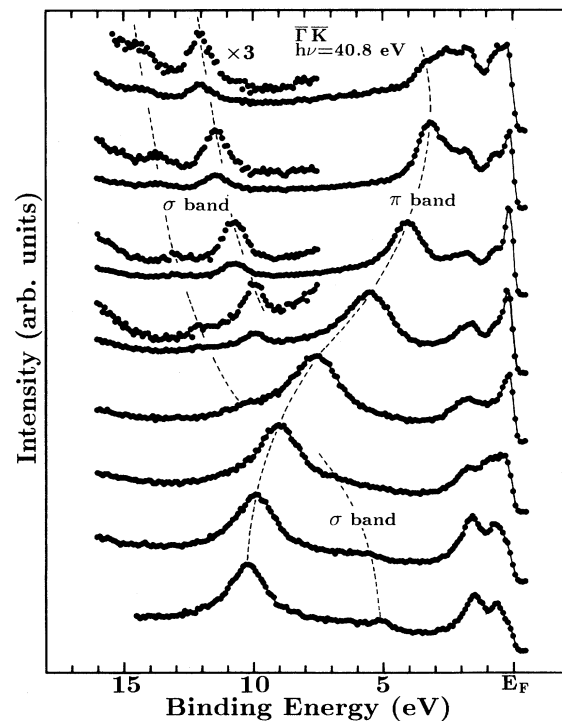


FIG. 6. Typical ARUPS spectra of MG/Ni(111) excited by the He II resonance line. The polar angle of emitted electrons is denoted for each spectrum.

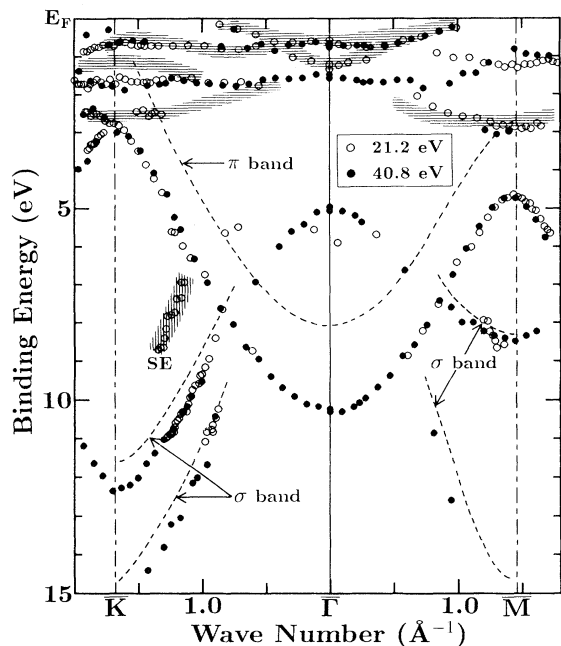


FIG. 7. Experimental band structure of MG/Ni(111). Shaded bands with horizontal lines near E_F indicate the dispersion relations of the d bands for the clean Ni(111) surface measured with He I. The experimental dispersion of bulk graphite (Ref. 6) is also indicated by broken curves for comparison. SE is an abbreviation for secondary electron.

bands of the MG agree fairly well with those of bulk graphite, the π band of MG lies at a much higher binding energy than the bulk one does. Second, for the isolated monolayer graphite film, the unoccupied antibonding π^* band is connected with the π band at the \bar{K} point.²⁶ Consequently, it may well be supposed that in MG on the Ni(111) surface the partially filled π^* band could be observed since the π band has a binding energy of 2.8 eV at the \bar{K} point as shown in Fig. 7. However, such a connection of the conduction band with the π band at the \bar{K} point has not been observed for MG/Ni(111). Instead, in the second Brillouin zone, we have detected one branch connected with the π band at the \bar{K} point, which could be a vestige of the severely deformed π^* band. Indeed, from the recent band-structure calculations of MG formed on the Ti-terminated TiC(111) surface, Kobayashi and Tsukada have pointed out that the π^* band is drastically deformed by hybridization with the substrate.²⁷ Therefore it is concluded that the π states, especially those with energies near E_F , are hybridized with the d states of the substrate, which leads to the formation of a covalent bond between the overlayer and the metal substrate.

This hybridization has also changed the dispersion of the energy bands of the substrate. In Fig. 7, the shaded bands with horizontal lines represent the dispersion of the clean Ni(111) surface observed with a photon energy of 21.2 eV. Although some branches of clean Ni(111) agree with those of MG-covered Ni(111), the one along

$\bar{\Gamma}\bar{K}$ at the energy of ~ 2 eV has disappeared upon the formulation of the graphite overlayer and an almost flat branch has appeared instead. This is additional evidence that the mixing of states with similar energies has taken place between the MG and the metal surface. Compared to this result, the difference in the band structure near E_F between the clean and BN-covered Ni(111) surfaces is small, as shown in Fig. 3. Therefore, together with the fact that the observed band structure of monolayer BN corresponds well with the theoretical one for bulk crystalline BN, we conclude that the bond between the BN film and the Ni(111) surface is weak compared to that between MG and the same substrate. This difference in the strength of the bond might appear in a difference in the interlayer distance between the overlayer and the substrate.²⁸ Some experiments concerning the surface structure such as LEED I - V analysis and ion-scattering spectroscopy are useful to test the above conclusion.

IV. SUMMARY

By using ARUPS and ARSEES, we have investigated the electronic dispersion relations of single-crystalline monolayer BN formed on the Ni(111) surface. The BN film prepared by the thermal decomposition of borazine on the substrate at 800°C did not grow in the layer-by-layer fashion after the formation of the first monolayer. In addition, because of the strong reduction of the surface reactivity due to the BN coating, the growth rate of the BN became extremely small after the first monolayer formation, which enabled one to obtain a well-prepared monolayer film. Of the five theoretical band structures,^{9,11-14} the one calculated by Catellani *et al.* has shown the best agreement with the present experimental band structure. This result demonstrates that a self-consistent band calculation with a sufficiently large basis set is necessary for describing precisely the electronic properties of BN. With the help of the theoretical band structure,¹⁴ the band gap in the BN film (E_G in eV) has been estimated to be $4.6 < E_G \lesssim 7$, which is comparable with the experimental values for the band gap in bulk BN reported so far.^{12,21-23} While the band structure of MG has been deformed strongly from that of bulk graphite by the mixing of the π states with the d states of the substrate, such substantial mixing has not taken place in the BN/Ni(111) system, which is ascribed to the absence of electronic states in the BN film with energies near E_F . Therefore it is concluded that the bond between the BN film and the Ni(111) surface is weak compared to that between MG and the same substrate.

ACKNOWLEDGMENTS

We would like to thank Professor M. Trenary of the University of Illinois at Chicago for suggesting the use of borazine for growing monolayer BN films and for a critical reading of the manuscript. One of the authors (A.N.) was supported by the Japan Society for the Promotion of Science.

- ¹S. P. S. Arya and A. D'Amico, *Thin Solid Films* **157**, 267 (1988).
- ²R. D. Leapman and J. Silcox, *Phys. Rev. Lett.* **42**, 1361 (1979).
- ³A. Mansour and S. E. Schnatterly, *Phys. Rev. B* **36**, 9234 (1987).
- ⁴R. C. Tatar and S. Rabii, *Phys. Rev. B* **26**, 4126; N. A. W. Holzwarth, S. G. Louie, and S. Rabii, *ibid.* **26**, 5382 (1982); H. J. F. Jansen and A. J. Freeman, *ibid.* **35**, 8207 (1987); J.-C. Charlier, X. Gonze, and J.-P. Michenaud, *ibid.* **43**, 4579 (1991).
- ⁵W. Eberhardt, I. T. McGovern, E. W. Plummer, and J. E. Fisher, *Phys. Rev. Lett.* **44**, 200 (1980); A. R. Law, J. J. Barry, and H. P. Hughes, *Phys. Rev. B* **28**, 5332 (1983); D. Marchand, C. Frétigny, M. Laguës, F. Battallan, Ch. Simon, I. Rosenman, and Pinchaux, *ibid.* **30**, 4788 (1984).
- ⁶T. Takahashi, H. Tokailin, and T. Sagawa, *Phys. Rev. B* **32**, 8317 (1985).
- ⁷Th. Fauster, F. J. Himpsel, J. E. Fischer, and E. W. Plummer, *Phys. Rev. Lett.* **51**, 430 (1983); I. Schäfer, M. Schlüter, and M. Skibowski, *Phys. Rev. B* **35**, 7663 (1987); F. Maeda, T. Takahashi, H. Ohsawa, S. Suzuki, and H. Suematu, *ibid.* **37**, 4482 (1988).
- ⁸E. Doni and G. Pastori Parravicini, *Nuovo Cimento B* **64**, 117 (1969).
- ⁹M. S. Nakhmanson and V. P. Smirnov, *Fiz. Tverd. Tela (Leningrad)* **13**, 3288 (1971) [*Sov. Phys. Solid State* **13**, 2763 (1972)].
- ¹⁰R. Dovesi, C. Pisani, and C. Roetti, *Int. J. Quantum Chem.* **17**, 517 (1980).
- ¹¹J. Zupan, *Phys. Rev. B* **6**, 2477 (1972).
- ¹²A. Zunger, A. Katzir, and A. Halperin, *Phys. Rev. B* **13**, 5560 (1976).
- ¹³J. Robertson, *Phys. Rev. B* **29**, 2131 (1984).
- ¹⁴A. Catellani, M. Posternak, A. Baldereschi, H. J. F. Jansen, and A. J. Freeman, *Phys. Rev. B* **32**, 6997 (1985); A. Catellani, M. Posternak, A. Baldereschi, and A. J. Freeman, *ibid.* **36**, 6105 (1987).
- ¹⁵E. Tegeler, N. Kosuch, G. Wiech, and A. Faessler, *Phys. Status Solidi B* **91**, 223 (1979).
- ¹⁶J. Barth, C. Kunz, and T. M. Zimkina, *Solid State Commun.* **36**, 453 (1980).
- ¹⁷A. Nagashima, K. Nuka, K. Satoh, H. Itoh, T. Ichinokawa, C. Oshima, and S. Otani, *Surf. Sci.* **287/288**, 609 (1993); A. Nagashima, K. Nuka, H. Itoh, T. Ichinokawa, C. Oshima, and S. Otani, *ibid.* **291**, 93 (1993).
- ¹⁸A. Nagashima, H. Itoh, T. Ichinokawa, C. Oshima, and S. Otani, *Phys. Rev. B* **50**, 4756 (1994).
- ¹⁹A. Nagashima, N. Tejima, and C. Oshima, *Phys. Rev. B* (to be published).
- ²⁰M. T. Paffett, R. J. Simonson, P. Papin, and R. T. Paine, *Surf. Sci.* **232**, 286 (1990); R. J. Simonson and M. Trenary, *J. Electron Spectrosc. Relat. Phenom.* **54/55**, 717 (1990); R. J. Simonson, M. T. Paffett, M. E. Jones, and B. E. Koel, *Surf. Sci.* **254**, 29 (1991).
- ²¹U. Büchner, *Phys. Status Solidi B* **81**, 227 (1977); C. Tarrío and S. E. Schnatterly, *Phys. Rev. B* **40**, 7852 (1989).
- ²²W. Baronian, *Mater. Res. Bull.* **7**, 119 (1977).
- ²³M. R. Vilanove, *C. R. Acad. Sci. Ser. B* **272**, 1066 (1972); D. M. Hoffman, G. L. Doll, and P. C. Eklund, *Phys. Rev. B* **30**, 6051 (1984).
- ²⁴T. R. Ohno, Y. Chen, S. E. Harvey, G. H. Kroll, J. H. Weaver, R. E. Haufler, and R. E. Smalley, *Phys. Rev. B* **44**, 13 747 (1991); T. Takahashi, S. Suzuki, T. Morikawa, H. Katayama-Yoshida, S. Hasegawa, H. Inokuchi, K. Seki, K. Kikuchi, S. Suzuki, K. Ikemoto, and Y. Achiba, *Phys. Rev. Lett.* **68**, 1232 (1992).
- ²⁵J. C. Phillips, *Bonds and Bands in Semiconductors* (Academic, New York, 1973).
- ²⁶G. S. Painter and D. E. Ellis, *Phys. Rev. B* **1**, 4747 (1970).
- ²⁷K. Kobayashi and M. Tsukada, *Phys. Rev. B* **49**, 7660 (1994).
- ²⁸From surface extended energy-loss fine-structure experiments, the interlayer distance between the MG and the Ni(111) surface has been estimated to be 2.80 Å. See R. Rosei, M. De Crescenzi, F. Sette, C. Quaresima, A. Savoia, and P. Perfetti, *Phys. Rev. B* **28**, 1161 (1983).